Absolute partial decay-branch measurements in 13C

Wheldon, Carl; Ashwood, Nicholas; Barr, Matthew; Curtis, Neil; Freer, Martin; Kokalova, Tzany; Malcolm, Jonathan; Ziman, Victor; Faestermann, Thomas; Wirth, Hans-Friedrich; Hertenberger, Ralf; Lutter, Rudi

DOI:
10.1103/PhysRevC.86.044328

Document Version
Early version, also known as pre-print

Citation for published version (Harvard):
Wheldon, C, Ashwood, N, Barr, M, Curtis, N, Freer, M, Kokalova, T, Malcolm, J, Ziman, V, Faestermann, T, Wirth, H-F, Hertenberger, R & Lutter, R 2012, 'Absolute partial decay-branch measurements in ^{13}C', *Physical Review C*, vol. 86, 044328, pp. 1-8. https://doi.org/10.1103/PhysRevC.86.044328

Absolute partial decay-branch measurements in ^{13}C

C. Wheldon,* N. I. Ashwood, M. Barr, N. Curtis, M. Freer, Tz. Kokalova, J. D. Malcolm, and V. A. Ziman
School of Physics and Astronomy, University of Birmingham, Edgbaston, Birmingham B15 2TT, United Kingdom

Th. Faestermann
Physik Department, Technische Universität München, D-85748 Garching, Germany

H.-F. Wirth, R. Hertenberger, and R. Lutter
Fakultät für Physik, Ludwig-Maximilians-Universität München, D-85748 Garching, Germany
(Received 29 June 2012; revised manuscript received 17 September 2012; published 22 October 2012)

The ^{9}Be(^{6}Li, d)^{13}C* reaction at a beam energy of 42 MeV has been investigated using a large-acceptance silicon-strip detector array and the high-resolution Q3D magnetic spectrograph. The Q3D facilitated the unambiguous determination of the reaction channel via identification of the deuteron ejectile, thereby providing the spectrum of excited states in ^{13}C in the range from 10.7 to 15.0 MeV. The silicon array was used to detect and identify the ^{13}C recoil-breakup products with efficiencies of up to 49%. The results obtained for the absolute partial branching ratios represent the first complete measurements for states in this energy region and allow the extraction of reduced widths. The quantities measured for $\Gamma_{n0}/\Gamma_{\rm tot}$ and $\Gamma_{n1}/\Gamma_{\rm tot}$ are 0.91 ± 0.11 and $\leqslant 0.13$ (10.753 MeV), 0.51 ± 0.04 and 0.51 ± 0.04 (10.818 MeV), 0.68 ± 0.03 and 0.42 ± 0.02 (10.996 MeV), 0.49 ± 0.08 and 0.71 ± 0.11 (11.848 MeV), and 0.49 ± 0.08 and 0.53 ± 0.08 (12.130 MeV), respectively. For the two observed higher-lying energy levels, $\Gamma_{\alpha 0}/\Gamma_{\rm tot}$ and $\Gamma_{n1}/\Gamma_{\rm tot}$ have been measured as 0.54 ± 0.02 and 0.45 ± 0.02 (13.760 MeV) and 0.94 ± 0.03 and 0.13 ± 0.02 (14.582 MeV), respectively. The consequences for the proposed molecular structures in ^{13}C are explored following the extraction of reduced widths.

DOI: 10.1103/PhysRevC.86.044328 PACS number(s): 21.10.−k, 24.10.Lx, 25.70.Hi, 27.20.+n

I. INTRODUCTION

Nuclear clustering is well established in light, α-conjugate nuclei [1] and as neutrons are added there is considerable evidence to suggest molecular configurations in which neutrons are shared between two (or more) heavier cores [2–5] appear. One of the most studied cluster nuclei is ^{12}C due to, mainly, the presence of the astrophysically important Hoyle state [6], and well-developed clustering has been observed. Beyond ^{12}C, bands involving molecular orbitals have been proposed in ^{13}C [7] starting at 9.9 MeV. These proposed structures consist of $K^{\pi} = \frac{3}{2}^{-}$ and $\frac{3}{2}^{+}$ bands and were obtained by systematically examining the properties of states via a detailed literature review and ordering those that do not exhibit shell-model character into bands, in some cases requiring spin and parity assignments quite different from the accepted values. In order to clarify the nature of states above the bandhead energy, the current study measures the decay branches—specifically, the partial decay branching ratios to states in daughter nuclei, which is one of the most useful properties when establishing the character of cluster states, enabling reduced widths to be extracted.

Here the absolute partial decay branches of states between 10.7 and 15.0 MeV in ^{13}C are measured. The relevant separation energies in ^{13}C are $S_n = 4.946$ MeV, $S_\alpha = 10.648$ MeV, and $S_p = 17.533$ MeV.

II. EXPERIMENTAL METHOD

A 42-MeV ^{6}Li^{3+} beam was provided by the 15-MV tandem Van de Graaff accelerator at the Maier-Leibnitz Laboratory (MLL) of the Technical and Ludwig-Maximillian Universities, Munich. The 4–10 electrical nano Amperes (enA) beam was incident on a 240 ± 40 μg cm^{-2} self-supporting ^{9}Be target. (The target was turned to $+28^{\circ}$ to face the two most forward positioned silicon detectors.) The ejectiles from the ^{9}Be(^{6}Li, d)^{13}C, α-transfer [8] reaction ($Q_0 = +9.174$ MeV) were detected using the high-resolution Q3D magnetic spectrograph [9] in combination with a position-sensitive proportional counter [10,11]. Energy and energy loss of the ions arriving at the focal plane were also measured, enabling the clear identification of deuterons. The properties of the Q3D are such that position along the focal plane corresponds to excitation energy in the recoiling nucleus, independent of angle. The breakup products from the recoiling ^{13}C nuclei were recorded using the Birmingham large-angular-acceptance position-sensitive silicon-strip detector array. Four 50×50 mm silicon-strip detectors, each with 16 horizonal and 16 vertical strips, were arranged in a 2×2 configuration spanning 12° to 91° and -36° to 39° in the horizontal and vertical planes, respectively. The master trigger condition required a Q3D focal-plane event, after which all Si analog-to-digital converter channels were read out using a 5-μs time window. Therefore, events corresponding to Q3D-only and Q3D+Si were obtained. More details on this setup can be found in Ref. [12] and references therein.

The Q3D focal-plane detector was calibrated by using known energies in ^{13}C and the presence of peaks from reactions on oxygen contaminants in the target. The Q3D was positioned

*c.wheldon@bham.ac.uk

at an angle of 20° for the majority of the measurements, but to unambiguously identify contaminant lines, a small amount of data at 30° were collected. The bulk of the data were taken at excitation energy settings of 11.550 (spanning 10.6 to 13. MeV) and 13.280 MeV (from 12.4 to 15.1 MeV) in the Q3D, with an intermediate energy of 12.187 MeV being used to track the states across the focal plane. Also, data at an energy setting of 6.864 MeV were recorded, from which the resolution of the Q3D with the energy loss through the ^{9}Be target was found to be 82 keV (after unfolding the 6-keV intrinsic width of the 6.864-MeV state [13]). This provides a lower limit on the resolution for the higher-energy settings, which correspond to lower deuteron energies and, therefore, can have marginally higher-energy straggling. A triple-α source (^{239}Pu, ^{241}Am, and ^{244}Cm) provided the silicon-detector energy calibration.

III. RESULTS

The data, dominated by single-hit events in the silicon-detector array, were sorted on an event-by-event basis [14], by reconstructing the kinematics for each open channel for the recoil in turn, namely, the ^{9}Be-α and ^{12}C-n channels for both the 11.550- and 13.280-MeV settings. In each case, reconstructing the second (lighter) breakup fragment using the detected particle, the deuteron, at the Q3D focal plane and two-body kinematics enables identification of both the recoil-breakup particles and their excitation energies. This was achieved via a Catania plot for each of the two breakup channels, by assuming the particle detected was the heavier of the two fragments. (More details can be found in Ref. [12].) This involved plotting the square of the missing momentum [of the reconstructed, undetected breakup particle, $p_2(tot)^2$] against the corresponding missing energy [of the reconstructed particle, $E_b - E_d - E_{1\mathrm{corr}}$] and noting that

$$E_b - E_d - E_{1\mathrm{corr}} = \frac{p_2(tot)^2}{2}\frac{1}{m_2} - Q_3, \qquad (1)$$

where E_b is the beam energy at the center of the target, E_d is the deuteron energy, and $E_{1\mathrm{corr}}$ is the energy of the detected recoil-breakup particle corrected for energy loss through the target and silicon-detector dead layer (0.3 μm Al). The result is a two-dimensional histogram for which the gradient of the loci is $1/m_2$ [the inverse of the mass (in atomic mass units) of the undetected particle] and the intercept is minus the three-body Q value, $-Q_3$. The Catania plots for the 11.550- and 13.280-MeV settings can be seen in Fig. 1.

In order to extract the detector efficiency for each registered particle and excitation energy, Monte Carlo simulations of the geometry using an isotropic breakup process have been performed using the RESOLUTION8 code [15,16]. Energy loss through the target and energy and angular straggling are included. The simulations were run for 1×10^5 Q3D focal-plane events for each particle at each energy setting and the efficiencies were derived. The resulting Catania plots using simulated data, plotted on the same intensity scale as the experimental statistics, are shown in Figs. 1(b) and 1(d). The efficiencies for detecting ^{12}C(g.s.), ^{12}C(2^+_1), and ^{9}Be(g.s.) are $\epsilon_{\mathrm{C(g.s)}} = 0.37 \pm 0.01$, $\epsilon_{\mathrm{C}(2^+_1)} = 0.41 \pm 0.01$, and $\epsilon_{\mathrm{Be(g.s)}} = 0.49 \pm 0.01$, respectively. The gates and sort code used to process the data were the same for both the simulated and real events.

The absolute partial decay branches were extracted using

$$\frac{\Gamma_{n0}}{\Gamma_{\mathrm{tot}}} = \frac{I(^{12}\mathrm{C(g.s.)})}{I(tot)\,\epsilon_{\mathrm{C(g.s)}}}, \quad \frac{\Gamma_{n1}}{\Gamma_{\mathrm{tot}}} = \frac{I(^{12}\mathrm{C}^*(2^+_1))}{I(tot)\epsilon_{\mathrm{C}(2^+_1)}},$$
$$\frac{\Gamma_{\alpha 0}}{\Gamma_{\mathrm{tot}}} = \frac{I(^{9}\mathrm{Be(g.s.)})}{I(tot)\epsilon_{\mathrm{Be(g.s)}}}, \qquad (2)$$

where $I(tot)$ is the total intensity at the Q3D focal plane. The spectra corresponding to the 11.550- and 13.280-MeV excitation energy settings are shown in Figs. 2 and 3, respectively, and the results are summarized in Table I. The areas under the Gaussian peaks and polynomial background were obtained using the BUFFIT fitting routine [17] and χ^2 minimization. Note that the focal plane was calibrated by fitting the energies from Ref. [13] to the peak centroids. The states populated are discussed in turn below, labeled by the centroid energies from Ref. [13].

A. 10.753 and 10.818 MeV

This doublet of states was observed by Aslanoglou *et al.* [18] using the same reaction as the present study, but at a ^{6}Li beam energy of 32 MeV. The width for the doublet (130 keV) is consistent with that observed here ($\approx$100 keV). The 10.753-keV state has $I^\pi = \frac{7}{2}^-$ [13,19] and a total $\Gamma_n/\Gamma_{\mathrm{tot}} = 0.70 \pm 0.10$ [13]. Note that from the literature it is not clear whether this total branch refers solely to the 10.753-MeV level or to the doublet. Hall and Bonner [20] have observed a 10.81-MeV resonance from inelastic neutron scattering on ^{12}C leading to the 2^+_1 state. The total width of 120 keV in Ref. [20] suggests that the doublet is populated. Here, the measured 10.753- and 10.818-MeV widths imply an experimental resolution of 86 keV, close to the measured value of 82 keV from the 6.864-MeV setting, largely from energy straggling in the beryllium target. The separation of the two centroids in the doublet is just below the full width at half maximum (FWHM) value of the resolution; nevertheless, from the inset of Fig. 2(c) it is clear that two components can be distinguished. Fitting with two Gaussians was necessary to well reproduce the peak shape, though the weaker population of the 10.753-MeV level leads to larger uncertainties for the branching ratios. The current measurement for the 10.753-keV state yields $\Gamma_n/\Gamma_{\mathrm{tot}} \leqslant 1.04 \pm 0.11$, comprising $\Gamma_{n0}/\Gamma_{\mathrm{tot}} = 0.91 \pm 0.11$ and $\Gamma_{n1}/\Gamma_{\mathrm{tot}} \leqslant 0.13$, to the ^{12}C ground and first excited states, respectively. The 10.818-MeV level has $I^\pi = (\frac{5}{2}^-)$ [13,21] with the assignment being consistent with an R-matrix analysis of neutron scattering data [22]. In the current study, the 10.818-MeV state is a factor of $\sim$10 more strongly populated than the neighboring 10.753-keV state. The absolute partial branching ratios measured here yield $\Gamma_n/\Gamma_{\mathrm{tot}} = 1.02 \pm 0.06$, comprising $\Gamma_{n0}/\Gamma_{\mathrm{tot}} = 0.51 \pm 0.04$ and $\Gamma_{n1}/\Gamma_{\mathrm{tot}} = 0.51 \pm 0.04$, to the ^{12}C ground and first excited states, respectively. These data represent the first complete absolute measurements for both components of the 10.8-MeV doublet and are as expected for these states, since

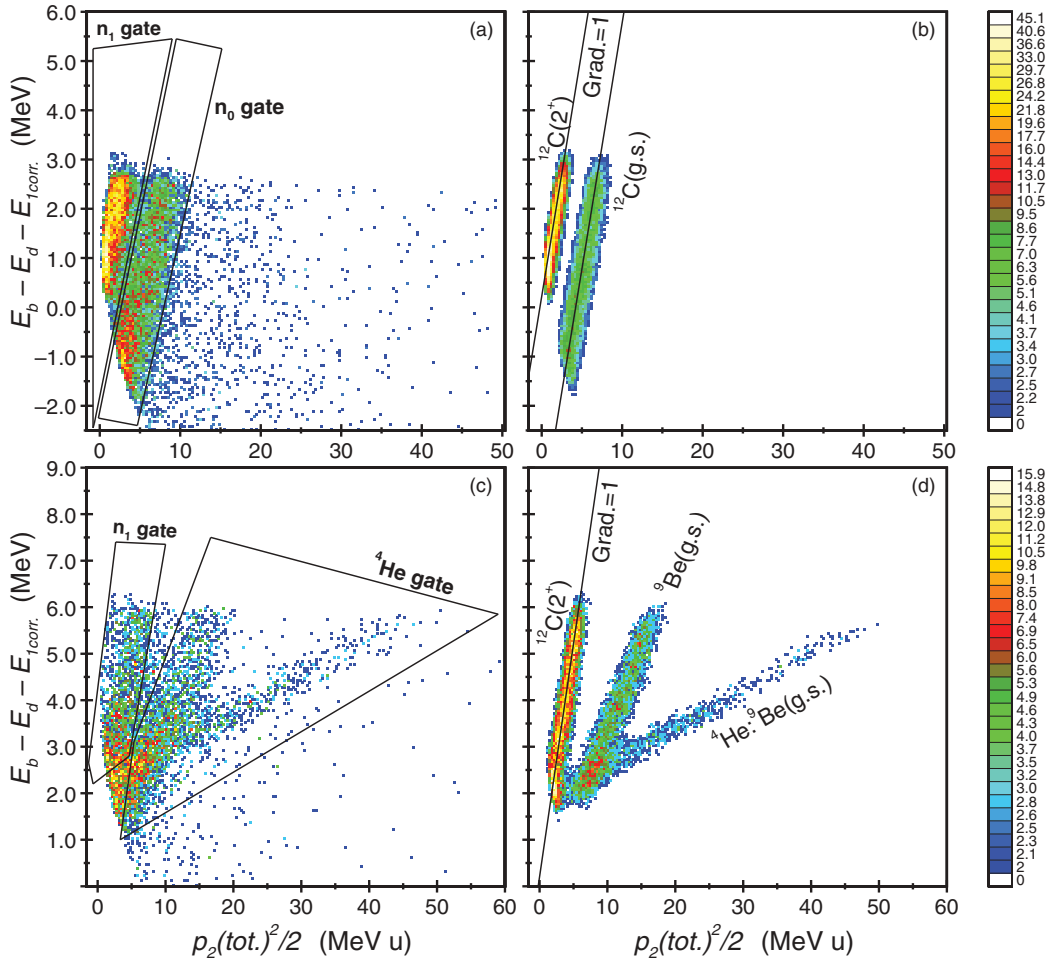

FIG. 1. (Color online) Particle identification (Catania) plots constructed by assuming the fragment registered in the silicon array is a ^{12}C nucleus. (a) Data for the Q3D setting centered at 11.550 MeV plotted for excitation energies between 10.60 and 11.30 MeV. The gates used to separate the ground- and first excited states of ^{12}C are shown. (b) Simulated events for the same excitation energy region. (c) Data for the 13.280-MeV setting with the gates for the neutron and α-breakup paths shown. (d) Simulated events for the 13.280-MeV setting labeled first by the particle detected in the silicon array. The lines on (b) and (d) have gradients = 1/1, demonstrating that the steepest distributions originate from reconstructing mass = 1 fragments (i.e., neutrons). The intensity scale for each pair of plots is shown on the right. A threshold condition of >1 has been applied to all of the plots to remove background counts.

the missing fraction of $1.0 - \Gamma_n/\Gamma_{\rm tot} = 0.3 \pm 0.1$ from the compiled value of the branching ratio cannot be from γ ray or α decay due to the location of the particle thresholds.

B. 10.996 MeV

This level is weakly populated in the current reaction and has a firm $I^\pi = \frac{1}{2}^+$ assignment [13,23]. The published value for the total neutron decay branch is 0.4 ± 0.1 [13], significantly below that measured here: $\Gamma_n/\Gamma_{\rm tot} = 1.10 \pm 0.04$, comprising $\Gamma_{n0}/\Gamma_{\rm tot} = 0.68 \pm 0.03$ and $\Gamma_{n1}/\Gamma_{\rm tot} = 0.42 \pm 0.02$. Once again, the measured branching ratio is close to the expected value of 1.0 for this state, in contrast to the compiled value. The width measured here for the 10.996-MeV state is significantly greater than that of 37(4) keV quoted in Ref. [13]. Removing the 82-keV experimental component from the measured width leads to an intrinsic state width of 85 keV for the 10.996-MeV state. It is noteworthy that an adjacent state at 11.080(5) MeV with $\Gamma_{\rm tot} = 4$ keV and $I^\pi = \frac{1}{2}^-$ [13] is not strongly populated [its position being indicated by the arrow in Fig. 2(a)], as the peak is well described by a single Gaussian component. Additionally, the focal-plane calibration is poor if an energy of 11.080 MeV is used instead of 10.996 keV.

C. 11.848 MeV and 12.13 MeV

The two states have spins and parities of $I^\pi = \frac{7}{2}^+$ and $\frac{5}{2}^-$, respectively [13], and have been measured here as part of a group of at least three broad resonances (see Fig. 2). The third, lower intensity peak, centered at 12.51 MeV, is most likely due to reactions on ^{16}O contaminants. Aslanoglou *et al.* [18] have observed the 11.848- and 12.13-MeV states with evidence for a similar (contaminant) peak at ~12.5 MeV (not labeled in Ref. [18]). The widths measured here for the 11.848- and 12.13-MeV states are somewhat larger

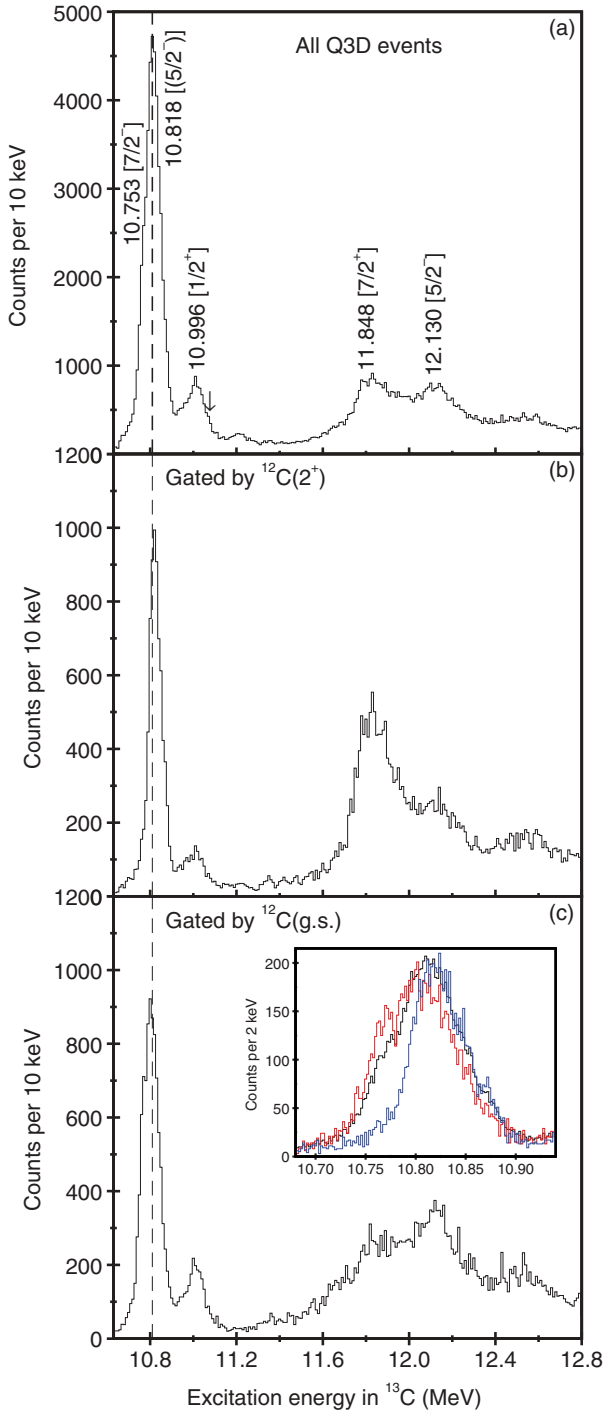

FIG. 2. (Color online) Spectra for the 11.550-MeV setting. (a) All Q3D events corresponding to deuteron ejectiles. The arrow indicates an energy of 11.080 MeV (see text for details). (b) Spectrum gated by the n_1 gate in Fig. 1(a); $^{12}C(2_1^+)$ state. (c) Spectrum gated by the n_0 gate in Fig. 1(a); ^{12}C ground state. The dotted line is to guide the eye and to discern the two components in the peak at 10.8 MeV. The inset of panel (c) shows the enlarged region around 10.8 MeV with 2 keV/channel (with 1/5 the compression as that for the main panel spectra): all Q3D events (black) with the vertical normalized to the blue spectrum; gated by $^{12}C(2^+)$ (blue); and gated by the ^{12}C ground state (red). Note that the original experimental dispersion from the focal-plane detector is ≈1 keV per channel.

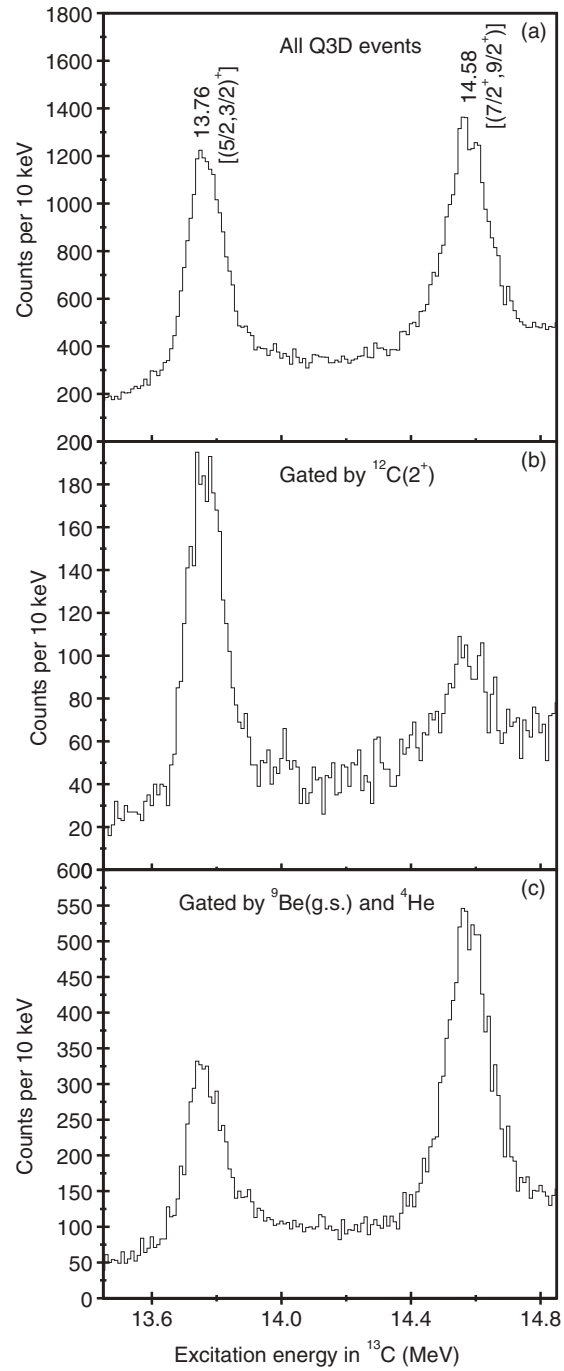

FIG. 3. Spectra from the 13.280-MeV setting. (a) All Q3D events corresponding to deuteron ejectiles. (b) Spectrum gated by the n_1 gate in Fig. 1(c); $^{12}C(2_1^+)$ state. (c) Spectrum gated by the ^{4}He gate in Fig. 1(c); ^{9}Be ground state.

than given in Ref. [13], but they are much closer to those measured by Hall and Bonner [20]: 260 and 200 keV, respectively. The published total neutron partial decay branch for the 12.13-MeV level is 0.43 ± 0.06 [13], which, in the absence of measured α-decay, implies a significant fraction of missing strength. In the current study, the total neutron partial

TABLE I. Absolute, partial neutron (part), and α-decay branching ratios measured in the present work and literature (lit) values. Upper limits for unobserved components appear in parentheses.

E_{level} (lit)[a] (MeV)	I^{π} [a]	Γ_{tot} (lit)[a] (keV)	E_{level} [b] (MeV)	FWHM[b] (keV)	Γ_{tot} [b]	$\Gamma_{part}/\Gamma_{tot}$ [b] ^{9}Be(g.s.)	^{12}C(g.s.)	^{12}C*(2_1^+)	$\Gamma_{part}/\Gamma_{tot}$ (lit) ^{9}Be(g.s.)	^{12}C(g.s.)	^{12}C*(2_1^+)
10.753(4)	$7/2^-$	55(2)	10.772	102(6)	61	(<0.05)	0.91(11)	$\leqslant$0.13		0.7(1)[a,c]	
10.818(5)	$(5/2^-)$	24(3)	10.816	89(2)	35	(<0.02)	0.51(4)	0.51(4)			
10.996(6)	$1/2^+$	37(4)	11.010	118(6)	85	(<0.08)	0.68(3)	0.42(2)		0.4(1)[a,c]	
11.848(4)	$7/2^+$	68(4)	11.841	252(42)	238	(<0.10)	0.49(8)	0.71(11)			
12.130(50)	$5/2^-$	80(30)	12.123	234(12)	219	(<0.17)	0.49(8)	0.53(8)		0.43(6)[a,c]	
13.760	$(5/2, 3/2)^+$	$\approx$300	(13.779)	143(4)	117	0.54(2)	(<0.10)	0.45(2)	0.30[d]	0.70[d]	0[d]
14.582(10)	$(7/2^+, 9/2^+)$	230(40)	(14.582)	154(4)	130	0.94(3)	(<0.12)	0.13(2)	0.86[d]	0.14[d]	0[d]

[a]From Ref. [13].
[b]Current work. The experimental resolution of 82 keV has been removed from the quoted Γ_{tot} values.
[c]Total neutron decay branching ratios.
[d]From Ref. [24].

decay branching ratios have been measured as 1.20 ± 0.14 (11.848 MeV), comprising $\Gamma_{n0}/\Gamma_{tot} = 0.49 \pm 0.08$ and $\Gamma_{n1}/\Gamma_{tot} = 0.71 \pm 0.11$, and 1.02 ± 0.13 (12.13 MeV), comprising $\Gamma_{n0}/\Gamma_{tot} = 0.49 \pm 0.08$ and $\Gamma_{n0}/\Gamma_{tot} = 0.53 \pm 0.08$. A large contribution to these uncertainties arises from the definition of the background in a region immediately below prominent contaminating peaks. Once again these results correspond to the first complete measurement for these states and are much closer to the anticipated value of $\approx$1.0 for the neutron branching ratios. The energy of the 12.130-MeV state is found here at 12.123 ± 0.004 MeV, with an additional systematic error of $\approx$10 keV due to the fitting procedure. Overall this is significantly lower than the 50-keV uncertainty quoted in Ref. [13].

There are several other known states around 12.1 MeV in the literature, but of these, the two closest to the 12.130 MeV level lie at 12.106 and 12.140 MeV and have published widths of 540 and 430 keV, respectively, significantly higher than the width of 234 keV measured here (although a small contribution to the observed spectrum at 12.1 MeV from a wide resonance cannot be ruled out). A state at 12.187(10) MeV with $\Gamma_{tot} = 150(40)$ keV [13] is the only possible alternative to the 12.13-MeV state, but this leads to a much larger χ^2 parameter when fitting the energies for the Q3D focal-plane calibration.

D. 13.760 and 14.582 MeV

The states observed here at 13.779 and 14.582 MeV have been assigned as the $I^{\pi} = (\frac{5}{2}, \frac{3}{2})^+$, $\Gamma \approx 300$ keV and $I^{\pi} = (\frac{7}{2}^+, \frac{9}{2}^+)$, $\Gamma \approx 230(40)$ keV levels [13]. The level energies are given in parentheses in Table I due to systematic uncertainties arising from bootstrapping the energy calibration from lower excitation energies. However, the energies assigned in Table I are the lowest possible energies for the states that are consistent with the properties of the focal plane. The measured partial branching ratios are 0.99 ± 0.03 (13.760 MeV), comprising $\Gamma_{\alpha 0}/\Gamma_{tot} = 0.54 \pm 0.02$ and $\Gamma_{n1}/\Gamma_{tot} = 0.45 \pm 0.02$, and 1.07 ± 0.04 (14.582 MeV), comprising $\Gamma_{\alpha 0}/\Gamma_{tot} = 0.94 \pm 0.03$ and $\Gamma_{n0}/\Gamma_{tot} = 0.13 \pm 0.02$. These are the only two states in the current work observed to decay via both neutron and α-particle breakup lying significantly above the α threshold. These measurements are the first model-independent partial decay branches for the 13.76- and 14.582-MeV levels.

Freer *et al.* [24] have performed an R-matrix analysis on states in this excitation energy region and conclude that the 13.76-MeV level has $I^{\pi} = \frac{5}{2}^+$ and a width of 337 keV, significantly more than the 143 keV measured here. The partial branching ratios in Ref. [24] are 0.30 and 0.70 for the α and neutron paths, respectively.

Although the numbers are not within one standard deviation the fact that there are large partial widths to both ^{9}Be and ^{12}C is consistent with the current results. The corresponding R-matrix results for the 14.582-MeV state [24] do not explicitly favor either $I^{\pi} = \frac{7}{2}^+$ or $\frac{9}{2}^+$, but the total width is 285 keV with $\Gamma_{\alpha 0}/\Gamma_{tot} = 0.86$ and $\Gamma_{n0}/\Gamma_{tot} = 0.14$, in very close agreement with the current results.

E. Above 14.582 MeV

Q3D settings of 14.6 and 15.8 MeV were used to explore excitation energies above the 14.582-MeV resonance but no structures have been observed. This was also the case for Aslanoglou *et al.* [18].

IV. DISCUSSION AND SUMMARY

In Sec. III precise measurements have been reported of the absolute partial branching ratios on a state-by-state basis. In the majority of cases these data represent the first measurement of all or most of the decay paths and their absolute intensities. However, due to the disproportionate effect that small (<1%) branching ratios can have on the interpretation of the underlying structure of a state, particularly near the barrier, a clearer view of the character of resonances is gained by calculating the reduced widths, γ_i^2, with the barrier penetrabilities, P_i, removed:

$$\gamma_i^2 = \frac{\Gamma_i}{2P_i}. \quad (3)$$

TABLE II. Barrier penetrabilities and reduced widths for states observed in the current work.

E_{level}(lit)	Γ_{tot}[a]	I^π	l			Branching ratios			Barrier penetrabilities[b]			Reduced widths[c]		
(MeV)	(keV)		$l_{\alpha 0}$	l_{n0}	l_{n1}	$\frac{\Gamma_{\alpha 0}}{\Gamma_{\text{tot}}}$	$\frac{\Gamma_{n0}}{\Gamma_{\text{tot}}}$	$\frac{\Gamma_{n1}}{\Gamma_{\text{tot}}}$	$P_{\alpha 0}$	P_{n0}	P_{n1}	$\theta^2_{\alpha 0}$	θ^2_{n0}	θ^2_{n1}
10.753	61	$7/2^-$	2	3	1	(<0.05)	0.91(11)	$\leqslant$0.13	0.0	0.20	0.56	–	0.019(4)	<0.002
10.818	35	$(5/2^-)$	2	3	1	(<0.02)	0.51(4)	0.51(4)	0.0	0.20	0.57	–	0.006(2)	0.004(1)
10.996	85	$1/2^+$	1	0	2	(<0.08)[c]	0.68(3)	0.42(2)	7.17×10^{-6}	1.00	0.14	<500	0.0038(4)	0.031(4)
11.848	238	$7/2^+$	3	4	2	(<0.10)[c]	0.49(8)	0.71(11)	0.0016	0.056	0.25	<4.21	0.13(3)	0.069(17)
12.130	219	$5/2^-$	2	3	1	(<0.17)	0.49(8)	0.53(8)	0.036	0.28	0.72	<0.27	0.024(4)	0.016(3)
(13.760)	117	$(5/2, 3/2)^+$	1	2	0	0.54(2)	(<0.10)	0.45(2)	0.50	0.67	1.00	0.022(1)	<0.0010	0.0041(3)
(14.582)	130	$(7/2^+, 9/2^+)$	3	4	2	0.94(3)	(<0.12)	0.13(2)	0.24	0.13	0.50	0.079(4)	<0.0057	0.0024(4)

[a]The experimental resolution of 82 keV has been removed from the widths measured in the current work (see Table I).
[b]The quantity $P_i/(k_i r_i) = 1/[F_l^2(k_i r_i) + G_l^2(k_i r_i)]$.
[c]Calculated using Γ_{tot} measured in the current work (column 2). See text for details.

The penetrabilities can be expressed in terms of the Coulomb wave function, $F_l(k_i r_i)$, and irregular Coulomb wave function, $G_l(k_i r_i)$, for the ith decay channel, wave number k_i, and radius $r_i = 1.4(A_{\text{recoil}}^{1/3} + A_i^{1/3})$ fm, such that $P_i = (k_i r_i)/[F_l^2(k_i r_i) + G_l^2(k_i r_i)]$. The orbital angular momentum carried by the decay particle is denoted by l. Substituting into Eq. (3) leads to

$$\gamma_i^2 = \Gamma_{\text{tot}} \frac{\Gamma_i}{\Gamma_{\text{tot}}} \frac{\left[F_l^2(k_i r_i) + G_l^2(k_i r_i)\right]}{2k_i r_i}. \tag{4}$$

Note that $\Gamma_i/\Gamma_{\text{tot}}$ are the measured branching ratios. Taking the ratio of the reduced width to the first Wigner sum rule [25,26] (also called the Wigner single-particle limit), where $\gamma_{Wi}^2 = 3\hbar^2/2\mu_i r_i^2$ and μ_i is the reduced mass of the recoil and decay particle, and substituting into Eq. (4) yields

$$\theta_i^2 = \frac{\gamma_i^2}{\gamma_{Wi}^2} = \Gamma_i \frac{2\mu_i r_i^2 \left[F_l^2(k_i r_i) + G_l^2(k_i r_i)\right]}{6\hbar^2 k_i r_i}, \tag{5}$$

as formulated in, e.g., Sanders *et al.* [27].

By examining the values shown in Table II, what is immediately clear is that a significantly lower limit can be placed on the α-particle branching ratio of the 10.996-MeV state such that the quantity $\theta_{\alpha 0}^2 \leqslant 1$. Taking the (lower) compiled value for the total width of 37 keV [13] results in a branching ratio of $\Gamma_{\alpha 0}/\Gamma_{\text{tot}} < 3.7 \times 10^{-4}$. Similarly, for the 11.848-MeV state, a slightly more stringent limit on the branching ratio of $\Gamma_{\alpha 0}/\Gamma_{\text{tot}} < 0.084$ is obtained.

From the reduced widths given in the final three columns of Table II the only significant α-particle strength for states above 11 MeV can occur for the 10.996-, 11.848-, and 12.13-MeV levels, the remaining populated states having $\theta_{\alpha 0}^2 < 10\%$. With the exception of the $I^\pi = (\frac{3}{2}^-)$ state at 13.280 MeV [13], reduced α decay widths for states in this energy region not observed in the current work cannot be calculated due to the absence of accurate branching ratio data. For the 13.280-MeV resonance, $\Gamma_{\alpha 0}/\Gamma_{\text{tot}} = 1.0$ and $\Gamma_{\text{tot}} = 340$ keV [13], which implies $\theta_{\alpha 0}^2 \approx 0.13$.

Examining the branching ratios to states in ^{12}C, one sees that there are no observed $n2$ decay branches to the Hoyle state [^{12}C(0_2^+), $E_x = 7.654$ MeV], despite the 13.760- and 14.582-MeV states lying above the threshold for such transitions: $S_{n2} = 12.600$ MeV. However, all the observed states fall below the $n3$ threshold at 14.587 MeV, corresponding to decays to the ^{12}C(3^-) level at $E_x = 9.641$ MeV. Assuming there is an unobserved branch from the 13.760-MeV state to the ^{12}C(0_2^+) and using a conservative upper limit of $\Gamma_{n2}/\Gamma_{\text{tot}} < 0.05$ leads to a reduced width of $\theta_{n2}^2 < 0.02$. Conversely, for the 14.582-MeV state a reduced width of $\theta_{n2}^2 = 1.0$ leads to a limit on the branching ratio of $\Gamma_{n2}/\Gamma_{\text{tot}} < 0.055$.

With no significant new α-cluster structures emerging from the reduced-width analysis, it is useful to remember that the (^{6}Li, d), α-transfer reaction used here is, in general, highly selective to states with strong α character [8]. It is indeed the case that the states populated here represent a rather selective subset of states, since the majority of resonances tabulated in this excitation energy regime have not been observed. Performing a semiclassical calculation to examine the difference in the incoming and outgoing angular momenta exposes a penchant for populating high-j (l) states in ^{13}C, with $\Delta L \approx 4.5\hbar$ for $E_x \approx$ 10-15 MeV. Although this broadly fits with the populated states listed in Table I, with the notable exception of the 10.996-MeV $I^\pi = \frac{1}{2}^+$ resonance, there are other high-j states in this region that have not been observed, e.g., the 12.438-MeV $I^\pi = \frac{7}{2}^-$ and 13.410-MeV $I^\pi = \frac{9}{2}^-$ [13] levels.

From earlier studies, spectroscopic factors for states in this energy regime have been published, such as those given in Table II of Ref. [18], also using the (^{6}Li, d) reaction, but at 32 MeV. Aslanoglou *et al.* [18] have reported a huge strength for the 10.75 + 10.82 MeV doublet, corresponding to $S_{\text{exp}} =$ 24.6. Qualitatively, this correlates with the population intensity observed in the current work. Using the same reaction, at a bombarding energy of 25.5 MeV, Rodrigues and co-workers [28] report that the doublet at 10.8 MeV also accounts for most of the observed strength. Where differences start to appear is in the higher-lying excitations close to 14 MeV. The current work and Refs. [18,28] all report markedly difference populations. This is most likely due to the different experimental conditions, in particular the large, $\theta = 20^\circ$ scattering angle used in the current study, by which the angular distributions change significantly [28].

The molecular-band states suggested by Milin and von Oertzen [7] are shown in Table III and span the excitation energy region elucidated here. The authors of Ref. [7] have

TABLE III. Proposed molecular-band levels in ^{13}C [7].

K^π [7]	E_{level}	I^π		Γ_{tot}
	(MeV)	Ref. [13]	Ref. [7]	(keV)
$\frac{3}{2}^-$	9.897	$\frac{3}{2}^-$	$\frac{3}{2}^-$	26
	10.818	$(\frac{5}{2}^-)$	$\frac{5}{2}^-$	24
	12.438	$(\frac{7}{2}^-)$	$\frac{7}{2}^-$	140
	14.130	$\frac{3}{2}^-$	$\frac{9}{2}^-$	∼150
	16.080	$(\frac{7}{2}^+)$	$\frac{11}{2}^-$	150
$\frac{3}{2}^+$	11.080	$\frac{1}{2}^-$	$\frac{3}{2}^+$	<4
	11.950	$(\frac{5}{2}^+)$	$\frac{5}{2}^+$	500
	13.410	$(\frac{9}{2}^-)$	$\frac{7}{2}^+$	35
	15.270	$\frac{9}{2}^+$	$\frac{9}{2}^+$	–
	16.950	–	$\frac{11}{2}^+$	330

performed a detailed review of all the states reported in the literature and examined their population in various categories of reactions. Based on this, together with energy systematics, bands with $K^\pi = \frac{3}{2}^-$ and $\frac{3}{2}^+$ have been proposed, extending from bandheads at 9.897 and 11.080 MeV, respectively, up to 16 MeV. According to Milin and von Oertzen [7], the states observed here fall predominantly into two categories. The 10.753-, 11.848-, 12.13-, and 13.760-MeV states have structures associated with a covalently bound neutron coupled with the ^{12}C(3$^-$) state (but the 14.582-MeV state has not been categorized). The 10.996-MeV state is associated with a neutron coupled to the Hoyle state: $^{12}\text{C}(0_2^+) \otimes 2s_{1/2}$. Finally, the 10.818-MeV state has a proposed $K^\pi = \frac{3}{2}^-$ molecular structure. Without additional information the overall picture that emerges from the states populated here is consistent with the lower molecular bands suggested in Ref. [7] in that the 10.818-MeV state is indeed strongly populated in α transfer and is a good candidate for a molecular-band member.

Finally, it is worth drawing attention to the fact that Freer *et al.* [24], in their recent R-matrix analysis, note that the narrow widths required (due to the centrifugal barrier) and the interference when including $I^\pi = \frac{9}{2}^-$ states below ≈16 MeV cause problems for the molecular-band interpretation of Ref. [7]. Specifically, this refers to the 14.130-MeV state in Table III. However, recently, following (^{6}Li, d) reactions, a newly observed narrow $L = 4$ resonance has been reported [28], albeit at the higher energy of 14.7 MeV. In the same study a narrow $L = 2$ resonance at 12.3 MeV is also reported, which may correspond to the $I^\pi = \frac{1}{2}^-$ resonance first described in Ref. [29]. This level has been proposed as a candidate for an α-cluster state.

By taking into consideration all of the aspects of the above discussion, it is clear that further experimental data in this energy regime are needed to firmly establish the molecular bands and to get a fully consistent picture of the structure of states in this region.

In summary, the ^{9}Be(^{6}Li, d)^{13}C* reaction has been studied at a bombarding energy of 42 MeV at the Technical and Ludwig-Maximillian Universities' tandem facility of the Maier Leibnitz Laboratory, Munich. The high-resolution Q3D magnetic spectrograph was used to select the deuteron ejectile, yielding ^{13}C excited states in the range from 10.7 to 15.0 MeV. An array of position-sensitive silicon detectors with large angular acceptance has measured the ^{13}C* breakup products, resulting in the measurement of absolute partial decay branching ratios for all of the populated states. These results represent the first complete and model-independent partial decay branches for all of the observed states. Reduced widths have been extracted and the results have been compared to the proposed molecular bands in ^{13}C.

ACKNOWLEDGMENTS

It is a pleasure to thank the accelerator operators of Maier-Leibnitz Laboratory for providing a stable ^{6}Li beam. Dr. Nicholas Keeley is thanked for useful discussions and performing distorted-wave Born approximation calculations. We acknowledge the financial support of the UK Science and Technology Facilities Council (STFC) and the DFG Cluster of Excellence 153, "Origin and Structure of the Universe." TzK is grateful for support by the Daphne Jackson Trust funded by the STFC.

[1] M. Freer, Rep. Prog. Phys. **70**, 2149 (2007).
[2] W. von Oertzen, M. Freer, and Y. Kanada-En'yo, Phys. Rep. **432**, 43 (2006).
[3] W. von Oertzen, Z. Phys. A **354**, 37 (1996); **357**, 355 (1997).
[4] M. Freer *et al.*, Phys. Rev. Lett. **82**, 1383 (1999).
[5] C. Wheldon *et al.*, Eur. Phys. J. A **26**, 321 (2005).
[6] F. Hoyle, D. N. F. Dunbar, W. A. Wenzel, and W. Whaling, Phys. Rev. **92**, 1095 (1953); C. W. Cook, W. A. Fowler, C. C. Lauritsen, and T. Lauritsen, *ibid.* **107**, 508 (1957).
[7] M. Milin and W. von Oertzen, Eur. Phys. J. A **14**, 295 (2002); Heavy Ion Phys. **18**, 171 (2003).
[8] H. W. Fulbright, Annu. Rev. Nucl. Part. Sci. **29**, 161 (1979).
[9] M. Löffler, H. J. Scheerer, and H. Vonach, Nucl. Instrum. Methods **111**, 1 (1973).
[10] H.-F. Wirth, H. Angerer, T. von Egidy, Y. Eisermann, G. Graw and R. Hertenberger, Beschleunigerlaboratorium München, Annual Report, 2000, p. 71.
[11] H.-F. Wirth, Ph.D thesis, Technical University, München, 2001; see http://tumb1.biblio.tu-muenchen.de/publ/diss/ph/2001/wirth.html.
[12] C. Wheldon *et al.*, Phys. Rev. C **83**, 064324 (2011).
[13] F. Ajzenberg-Selove, Nucl. Phys. A **523**, 1 (1991).
[14] C. Wheldon, http://www.wheldon.talktalk.net/files/munich_decoder.c.
[15] N. Curtis *et al.*, Phys. Rev. C **51**, 1554 (1995).
[16] N. Curtis *et al.*, Phys. Rev. C **53**, 1804 (1996).
[17] N. M. Clarke, Birmingham University Fast FITting (BUFFIT) version 4.8, 1998, part of the Sunsort analysis software, http://npg.dl.ac.uk/Charissa/documents/CODES/sunsort/.
[18] X. Aslanoglou, K. W. Kemper, P. C. Farina, and D. E. Trcka, Phys. Rev. C **40**, 73 (1989).
[19] F. Ajzenberg-Selove, Nucl. Phys. A **152**, 1 (1970).
[20] H. E. Hall and T. W. Bonner, Nucl. Phys. **14**, 295 (1959).
[21] F. Ajzenberg-Selove, Nucl. Phys. A **268**, 1 (1976).

[22] H. D. Knox and R. O. Lane, Nucl. Phys. A **378**, 503 (1982).
[23] F. Ajzenberg-Selove, Nucl. Phys. A **360**, 1 (1981).
[24] M. Freer *et al.*, Phys. Rev. C **84**, 034317 (2011).
[25] R. Nilson, W. K. Jentschke, G. R. Briggs, R. O. Kerman, and J. N. Snyder, Phys. Rev. **109**, 850 (1958).
[26] T. Teichmann and E. P. Wigner, Phys. Rev. **87**, 123 (1952).
[27] S. J. Sanders, L. M. Martz, and P. D. Parker, Phys. Rev. C **20**, 1743 (1979).
[28] M. R. D. Rodrigues *et al.*, AIP Conf. Proc. **1245**, 141 (2010); **1351**, 125 (2011); and T. Borello-Lewin *et al.*, Int. J. Mod. Phys. E **20**, 1018 (2011).
[29] T. Kawabata *et al.*, J. Phys.: Conf. Ser. **111**, 012013 (2008).